

---

1 **Over 50000 metagenomically assembled draft genomes for the**  
2 **human oral microbiome reveal new taxa**

3 Jie Zhu<sup>1,2,‡</sup>, Liu Tian<sup>1,2,‡</sup>, Peishan Chen<sup>1,3</sup>, Mo Han<sup>1,4</sup>, Liju Song<sup>1,2</sup>, Xin Tong<sup>1,2</sup>,  
4 Zhipeng Lin<sup>1</sup>, Xing Liu<sup>1</sup>, Chuan Liu<sup>1</sup>, Xiaohan Wang<sup>1</sup>, Yuxiang Lin<sup>1</sup>, Kaiye Cai<sup>1</sup>,  
5 Yong Hou<sup>1</sup>, Xun Xu<sup>1,2</sup>, Huanming Yang<sup>1,5</sup>, Jian Wang<sup>1,5</sup>, Karsten Kristiansen<sup>1,4</sup>,  
6 Liang Xiao<sup>1,3,6</sup>, Tao Zhang<sup>1,4</sup>, Huijue Jia<sup>1,2,9,\*</sup> & Zhuye Jie<sup>1,2,4,\*</sup>

7

8 <sup>1</sup> BGI-Shenzhen, Shenzhen 518083, China

9 <sup>2</sup> Shenzhen Key Laboratory of Human Commensal Microorganisms and Health  
10 Research, BGI-Shenzhen, Shenzhen 518083, China

11 <sup>3</sup> Shenzhen Engineering Laboratory of Detection and Intervention of human intestinal  
12 microbiome

13 <sup>4</sup> Laboratory of Genomics and Molecular Biomedicine, Department of Biology,  
14 University of Copenhagen, DK-2100 Copenhagen, Denmark

15 <sup>5</sup> James D. Watson Institute of Genome Sciences, Hangzhou 310058, China

16 <sup>6</sup> BGI-Qingdao, BGI-Shenzhen, Qingdao, 266555, China

17 <sup>‡</sup> These authors contributed equally to this work

18 \*Correspondence should be addressed to Z.J. [jiezhuye@genomics.cn](mailto:jiezhuye@genomics.cn), H.J.  
19 [jiahuijue@genomics.cn](mailto:jiahuijue@genomics.cn).

20

21 **ABSTRACT**

22 **The oral cavity of each person is home for hundreds of bacterial species. While**  
23 **taxa for oral diseases have been well studied using culture-based as well as**  
24 **amplicon sequencing methods, metagenomic and genomic information remain**  
25 **scarce compared to the fecal microbiome. Here we provide metagenomic shotgun**  
26 **data for 3346 oral metagenomics samples, and together with 808 published**  
27 **samples, assemble 56,213 metagenome-assembled genomes (MAGs). 64% of the**  
28 **3,589 species-level genome bins contained no publicly available genomes, others**

---

29 **with only a handful. The resulting genome collection is representative of samples**  
30 **around the world and across physiological conditions, contained many genomes**  
31 **from Candidate phyla radiation (CPR) which lack monoculture, and enabled**  
32 **discovery of new taxa such as a family within the Acholeplasmataceae order.**  
33 **New biomarkers were identified for rheumatoid arthritis or colorectal cancer,**  
34 **which would be more convenient than fecal samples. The large number of**  
35 **metagenomic samples also allowed assembly of many strains from important**  
36 **oral taxa such as *Porphyromonas* and *Neisseria*. Predicted functions enrich in**  
37 **drug metabolism and small molecule synthesis. Thus, these data lay down a**  
38 **genomic framework for future inquiries of the human oral microbiome.**

39

40 The human microbiome has been implicated in a growing number of diseases.  
41 The majority of microbial cells is believed to reside in the large intestine<sup>1</sup> and cohorts  
42 with fecal metagenomic data contain over 1000 individuals<sup>2,3</sup>. For the oral  
43 microbiome, hundreds of metagenomic shotgun-sequenced samples have been  
44 available from the Human Microbiome Project (HMP) and for rheumatoid arthritis<sup>4-6</sup>.  
45 A number of other diseases studied by Metagenome-wide association studies (MWAS)  
46 using gut microbiome data also indicated potential contribution from the oral  
47 microbiome in disease etiology<sup>7-12</sup>. Although the MWAS on rheumatoid arthritis was  
48 based on a *de novo* assembled reference gene catalog for the oral microbiome<sup>6</sup>,  
49 analyses on bacterial genomes would be more desirable. And when oral samples show  
50 comparable or better sensitivity and accuracy for disease diagnosis, prognosis or  
51 patient stratification than fecal samples, oral samples would be much more convenient  
52 as they could be available at any time and taken at a fully controlled setting witnessed  
53 by trained professionals. Unlike the anaerobic environment for the gut microbiome,  
54 the oral microbiome is believed to be well covered by culturing<sup>13</sup>, and analyses by  
55 16S rRNA gene amplicon sequencing or polymerase chain reaction (PCR) are  
56 common. Recently published large-scale metagenomic assembly efforts mostly

57 included fecal metagenomic data<sup>14-16</sup>. It is not clear how much is really missing for  
58 the oral microbiome. The saliva, in particular, seems to have more bacterial species  
59 per individual than the fecal microbiome<sup>17</sup>.

60 After getting contigs using assembly algorithms suitable for metagenomic  
61 data<sup>18</sup>, a central idea used by metagenomic binning algorithms is that genes or contigs  
62 that co-vary in abundance among many samples belong to the same microbial  
63 genome<sup>8, 19-21</sup>. Large cohorts are therefore prerequisites for high-quality assembly.

64 Here we present 3346 new oral metagenomic samples, and 56,213  
65 metagenome-assembled genomes (MAGs) which represent 3,589 species-level clades,  
66 revealing new taxa as well as substantially complementing the genomic content of  
67 known species. This genome reference are highly representative of metagenomic  
68 samples not used in assembly, and could facilitating culturing, functional screens as  
69 well as disease diagnosis and modulation based on the oral microbiome.

## 70 **RESULTS**

### 71 **Draft genomes assembled from oral metagenomic data**

72 In order to substantially increase the amount of oral microbiome data, we  
73 shotgun sequenced 2284 saliva and 391 tongue dorsum samples from the 4D-SZ  
74 cohort<sup>3, 12, 22</sup>, 671 saliva samples from five ethnic groups of Yunnan province,  
75 producing over 43.19 terabytes of sequence data (**Supplementary Table 1**). Together  
76 with 808 published samples from 5 studies<sup>6, 23-26</sup> that have not been used for  
77 metagenomic assembly (**Supplementary Table 1**), a total of 4,154 oral samples with  
78 metagenomic data were obtained. The data in each sample was single assembled into  
79 contigs using SPAdes<sup>27, 28</sup> (**Fig. 1a, Supplementary Table 1**). Binning was then  
80 performed using MetaBAT2<sup>21</sup> for the 39,458,119 contigs longer than 1.5kb, leading to  
81 56,213 metagenome-assembled genomes (MAGs), 15,013 of which were of high  
82 quality according to recently agreed standards<sup>29</sup> using CheckM<sup>30</sup> (>90% completion,  
83 <5% contamination, **Fig. 1a**). The remaining 41,200 also reached the standards for

---

84 medium-quality MAGs (>50% completion, <10% contamination), while low-quality  
85 assemblies were not further analyzed (**Supplementary Table 2**). The median  
86 constructed MAGs per sample is 12, with highest from ZhangX\_2015  
87 (**Supplementary Figure 1a**).

### 88 **New genomes from the new samples**

89 To evaluate the novelty of the assembled genomes, delineate their taxonomy  
90 and potential source, we comprehensively incorporated 190,309 existing isolate or  
91 metagenome-assembled genomes from NCBI Refseq, eHOMD<sup>31</sup> (the expanded  
92 Human Oral Database), and recent publications<sup>14-16, 32</sup> including our culture collection  
93 from fecal samples in Shenzhen<sup>33</sup> (**Fig. 1a**).

94 Species-level clusters (SGBs, for species-level genome bins) were computed  
95 for the over 0.25 million genomes following multiple steps (**Fig. 1a**, see Methods for  
96 details), defined as at least 95% average nucleotide identity (ANI) and at least 30%  
97 overlap of the aligned genomes. The clustering well-collapsed the genomes, with  
98 about 10-fold reduction in number, i.e. resulting in around thirty thousand species.  
99 Besides the 27,936 species that were non-oral according to reference genomes in the  
100 cluster (defined in **Fig. 1b**), 2,313 clusters (64% of the total oral species) only  
101 contained our MAGs (denoted uSGBs for unknown SGBs), some of which were  
102 repeatedly captured in our data, with more than 50 genomes each (**Fig. 1b,c**); the  
103 1,276 known oral SGBs (kSGBs) could be further divided according to the percentage  
104 of reference genomes in the cluster. Interestingly, kSGBs with over 50% unknown  
105 genomes outnumbered kSGBs with 0-50% unknown genomes for clusters containing  
106 10 or more genomes (**Fig. 1b,c**), underscoring the discovery power of large  
107 metagenomic cohorts. And the top three contributions of uSGBs are 4D\_SZ (1441),  
108 ZhangX\_2015 (445) and Yunnan (334) (**Supplementary Figure 1b**). Comparing the  
109 ratio of new MAGs in the samples, we retrieved a greater fraction of previously  
110 unknown genomes in dental compared to saliva or tongue samples, even though we

111 did not take dental samples for this large cohort (**Fig. 1d**). This ratio also appeared to  
112 differ between cohorts, with less than 10% unknown for samples from France or the  
113 U.S., and more newly matched uSGBs for samples from Fiji, Germany and  
114 Luxemburg (**Fig. 1d**). The large cohort available from this study is crucial for the  
115 retrieval of novel oral species, contributing over 2000 uSGBs, greatly expanding our  
116 knowledge of oral microbiome diversity.

### 117 **Close to 90% representation of oral metagenomics data by the genomes**

118 We next examined the ability of this species-level genomes set to represent  
119 metagenomic shotgun data. We assessed the percentage of reads that could align to  
120 cultured genomes only (eHOMD) and cultured complemented by metagenomically  
121 assembled genomes. The median was 66.99% mapping with the 1526 genomes from  
122 eHOMD (**Fig. 2a**). The 4930 representative human SGBs from a recent large-scale  
123 assembly study that included available oral metagenomic samples<sup>16</sup> led to 79.72%  
124 mapping, and the representative oral 3589 SGBs from the current study instead led to  
125 88.06% mapping (median for all samples), especially for metagenomes from the U.S.  
126 and Germany; and a median of 85.29% mapping even for 81 saliva and subgingival  
127 metagenomes from three cohorts that were not used in the assembly process<sup>34-36</sup> (**Fig.**  
128 **2a, Supplementary Table 1**). Across physiological states, our SGBs well represented  
129 pregnant samples from the U.S. (reaching 92.99% mapping), RA (reaching 90.69%  
130 mapping) and diabetes (reaching 83.99% mapping) (**Fig. 2b**). Such a high degree of  
131 representation of metagenomic data across geography, ethnicity, age and  
132 physiological states suggest that the expanded genomic content of oral SGBs could  
133 serve as a starting point for quantitative taxonomic and functional analyses of the  
134 human oral microbiome.

### 135 **Taxonomic landscape of the oral microbial genomes**

136 We constructed a phylogenetic tree for the 3,589 oral SGBs, and similar to the  
137 gut microbiome, *Firmicutes* took up the largest number of branches (1248 clusters,

---

138 12307 genomes, **Fig. 3c**). The other 46276 genomes distributed into 15 phyla,  
139 including major human oral phyla such as *Actinobacteria* (490 SGBs, 6477 genomes),  
140 *Bacteroidetes* (368 SGBs, 23409 genomes), *Proteobacteria* (364 SGBs, 7570  
141 genomes), *Campylobacteriota* (280 SGBs, 1841 genomes), and *Fusobacteriota* (145  
142 SGBs, 1998 genomes) (**Fig. 3, Supplementary Table 3**). uSGB accounted for 181.27%  
143 increase in the reconstructed phylogenetic branch length, with over 80% of the  
144 diversity in *Campylobacterota* phylum contributed by the new uSGBs, follow by over  
145 70% for *Patescibacteria* and *Fusobacteriota* (**Fig. 3b**), which seemed overlooked by  
146 culturing studies. We estimated there is median of 210 SGBs with the relative  
147 abundance higher than 0.001 per sample (**Supplementary Figure 1c**). Besides uSGB  
148 are also very high abundance, explained for 68.10% of richness and 65.23% of  
149 relative abundance per sample (**Supplementary Figure 1d,e**). Our MAGs greatly  
150 expanded the species or strains diversity within each phylum. As many as 596 SGBs  
151 from 4006 genomes belonged to the candidate superphylum of *Patescibacteria*  
152 (*Parcubacteria*, also known as OD1), which only have 157 kSGB with 3115 reference  
153 genomes. We note a few not so well studied phyla that were interesting in analogy to  
154 the gut microbiome. *Akkermansia* is the only genus from Verrucomicrobiota in the  
155 human gut and intensively pursued for its role in health and diseases, and  
156 Verrucomicrobiota and Spirochaetota take up a greater fraction in Hadza hunter  
157 gatherers compared to developed countries<sup>37</sup>. Here we identified 6 genomes in 3  
158 SGBs for Verrucomicrobiota, and 900 genomes in 67 SGBs for Spirochaetota. 121  
159 reference genome was only available for 32 SGB within Spirochaetota. 198 SGBs  
160 with 1169 genomes belong to the candidate division Saccharibacteria (TM7) (**Fig. 3a,**  
161 **Supplementary Table 3**).

162 At the genera level, *Streptococcus*(460 SGBs), *Campylobacter*(279 SGBs),  
163 *Actinomyces*(184 SGBs), *Prevotella*(159 SGBs), *Atopobium*(146 SGBs) were the  
164 major genera in the SGBs(**Supplementary Table 3**). 265 of the 2313 uSGBs had  
165 taxonomic information until order or family, but cannot be annotated to a known

---

166 genus. The top three uSGB classified families were Saccharimonadaceae (17.99%),  
167 Streptococcaceae (12.88%) and Campylobacteraceae (9.51%), whereas the most  
168 assigned genera were Streptococcus (12.88%), Campylobacter\_A (7.65%) and TM7x  
169 (5.92%) (**Fig. 3c**).

#### 170 **A new family with small genomes**

171 In the Achleplasmatales order (Mollicutes class) of the *Tenericutes* phylum, a  
172 number of our uSGBs with high-quality MAGs formed a clade distinct from  
173 *Acheloplasma* and *Candidatus Phytoplasma*, with shallow branches within the clade  
174 (**Fig. 4a**). The genome size of this genome-defined family, which we temporarily  
175 denoted as *Ca. Bgiplasma*, is  $0.69\pm 0.05$  Mbp, which is similar to *Candidatus*  
176 *Phytoplasma* ( $0.64\pm 0.14$  Mbp), but much smaller than *Acheloplasma* ( $1.50\pm 0.20$   
177 Mbp). Genomes of such small size were discarded in early efforts of metagenomic  
178 assembly<sup>19</sup>, but we now know *Ca. Bgiplasma* are complete entities according to  
179 single-copy marker genes in CheckM (**Supplementary Table 2**). The GC content of  
180 the three clades were also different. *Ca. Bgiplasma* family was more towards normal  
181 GC content ( $34.57\pm 0.21\%$ ), not as low as *Acheloplasma* ( $30.99\pm 1.75\%$ ) and  
182 *Candidatus Phytoplasma* ( $25.98\pm 2.68\%$ ) (**Supplementary Table 5**). Despite the lack  
183 of deep branches, the ANI distribution of uSGB within *Ca. Bgiplasma* family showed  
184 two separate groups at genus-level divergence (ANI <85%) (**Fig. 4b**), illustrating  
185 diversity within this new family. This 11 uSGBs comprising 29 MAGs contribute  
186 more than 0.1% relative abundance in 209 samples, indicating that this family is an  
187 potentially important but so far uncharacterized clade in the oral microbiome.

188 5.53 M genes (87.97% of total) of representatives genome of SGBs can be  
189 annotated by EggNOG mapper<sup>38, 39</sup> with the rate of annotation 89.55% for uSGBs and  
190 81.83% for *Ca. Bgiplasma* family (**Supplementary Table 5**). We found *Ca.*  
191 *Bgiplasma* are gene content dominated by replication, recombination and repair,  
192 posttranslational modification, protein turnover, chaperones, and inorganic ion

---

193 transport and metabolism, which are reported active up-regulated in *Deinococcus*  
194 during gamma-irradiation<sup>40</sup> (**Supplementary Fig. 2b**).

### 195 **Distribution of species and strains**

196 The new samples from this study differed in oral microbiome composition  
197 compared to published samples across geography/ethnicity (**Fig. 5a,b**). Both the  
198 4D-SZ and Yunnan samples abundantly contained many uSGBs (of the top 10  
199 abundance species in cohort) such as *Neisseria* spp., *Porphyromonas* spp. and kSGBs  
200 such as *Haemophilus parainfluenzae* and *Veillonella denticarios*, which were rare in  
201 the other cohorts (**Fig. 5b**). Pregnant samples from the U.S. contained *Fannyhessea*  
202 *vaginae* (the vaginal pathogen previously known as *Atopobium vaginae*<sup>41</sup>),  
203 *Urinacoccus*, etc. that were of much lower abundance in other cohorts (**Fig. 5b**).  
204 Samples from Fiji, although not well mapped (**Fig. 2a**), showed high levels of a few  
205 SGBs that were also seen in the RA study from Beijing, China, including an SGB  
206 from *Saccharibacteria* (TM7) (**Fig. 5b**).

207 At the strain level, the new samples from the current study greatly expanded  
208 the genome collection for common taxa such as *Neisseria* spp., *Porphyromonas* spp.,  
209 and *Prevotella* spp. (**Fig. 5c,d**). The numbers of publicly available reference genome  
210 for the top ten most abundant species in the genera *Porphyromonas* and *Prevotella*  
211 were less than 10, and less than 100 for the genus *Neisseria*. Here we obtained more  
212 than 1000 genomes for a few of the species, and increased the diversity in all the  
213 species in these genera (**Fig. 5c**). Most of the species with a large number of genomes  
214 showed strain-level variations (subspecies). The *Prevotella nanceiensis* kSGB, for  
215 example, included 3 reference genomes that were similar to a few genomes from  
216 developed countries, while our samples contributed two large clusters that were more  
217 distantly related (**Fig. 5d**).

### 218 **New disease markers according to the oral genomes**



---

219 To illustrate the utility of our genome collection in metagenomic studies  
220 including MWAS, we reanalyzed dental and salivary microbiome data from RA  
221 patients and controls<sup>6</sup>. For better confidence in the markers regardless of cohort, we  
222 only analyzed SGBs containing >10 genomes. Similar to the original study, oral  
223 markers selected by a 5x 10-fold cross-validated gradient boosting algorithm  
224 include a number of Gram-negative bacteria e.g. *Haemophilus* spp.,  
225 *Aggregatibacter* spp. enriched in dental samples from healthy volunteers, while  
226 only a *Pseudomonas* SGB and a *Enterococcus* SGB were selected for RA samples  
227 (**Fig. 6a**). Interestingly, the two new RA dental markers appeared more abundant in  
228 control saliva samples. The strongest marker from healthy saliva remained  
229 *Lactococcus lactis*<sup>5</sup>, and *Lactobacillus paracasei*, *Streptococcus infantarius*, were  
230 identified, reminiscent of beneficial effects of *L. casei* gavage in rat model of RA<sup>42</sup>.  
231 <sup>43</sup>. The assembled genomes allowed matching of different species in the *Veillonella*  
232 genus as RA saliva markers. Moreover, *Pauljensenia* spp., a genus recently renamed  
233 from *Actinomyces*<sup>44</sup>, was identified as highly predictive of RA. As *Actinomyces* are  
234 the basis for dental attachment of oral bacteria<sup>45</sup>, potential contribution of  
235 *Pauljensenia* spp. to periodontitis in RA patients remains to be explored; the dental  
236 microbiome was obviously deranged, consistent with epidemiology<sup>5</sup>.

237 A set of saliva samples from colorectal cancer and controls from France are  
238 also available<sup>46</sup>. Here, we found *Pauljensenia* spp., to be control-enriched, along with  
239 *Acinetobacter radioresistens*, *Lachnoanaerobaculum* sp., *Catonella* sp., etc (**Fig. 6b**).  
240 *Streptococcus thermophilus*, a species previously found to be enriched in fecal  
241 samples from control or adenoma compared to CRC patients<sup>47</sup> was also identified in  
242 control saliva. The markers enriched in CRC oral samples are more unexpected.  
243 Besides *Porphyromonas* spp., *Prevotella maculosa*, we found a *Lachnospiraceae*  
244 SGB (potentially TMA-producing and consistent with gut results<sup>10, 48-50</sup>),  
245 *Capnocytophaga leadbetteri*, *Cardiobacterium hominis*, etc. (**Fig. 6b**). Thus, the  
246 substantially expanded collection of oral microbial genomes enabled discovery of new

247 disease markers and genomic representation of previously reported markers,  
248 facilitating the shift from fecal to oral microbiome-based diagnosis and therapeutics.

### 249 **Potential functions in drug metabolism and small molecule synthesis**

250 Many human target drugs are reported to be metabolized to its inactive form  
251 by gut human microbiome<sup>51, 52</sup> or impact the gut bacteria<sup>51-53</sup>. Gut bacteria genes that  
252 metabolize 41 human targeted drugs, 6 non-traditional antibacterial therapeutic and  
253 key enzymes experimentally validated for 12 human diseases were mapped to our oral  
254 SGB genomic contents (**Supplementary Tables 6**). We show that many oral  
255 communities share homologous to these gut bacteria encoding enzymes, suggesting  
256 the oral microbiome may also play an important role in medical therapy and disease  
257 development (**Fig. 7a**). More specifically, there are total 2696 SGBs contain  $\beta$   
258 -glucuronidase enzyme that can metabolize anti-cancer drug Gemcitabine (2',  
259 2'-difluorodeoxycytidine) into its inactive form<sup>52</sup>. 456 SGBs have agmatine gene for  
260 anti-T2D drug Metformin and 225 SGBs have tyrosine decarboxylase (TyrDC) for  
261 anti-parkinson drug L-dopa<sup>51</sup>. There are also 1733 oral SGBs have genes producing  
262 small molecule taurine and 5-aminovaleurate which are potential drugs for autism  
263 spectrum disorder (ASD)<sup>51</sup>. Unexpectedly few SGBs contain CutC/CutD genes which  
264 are key enzymes for TMA, a metabolite with high cardiovascular event risk<sup>51</sup>.

265 The inference of secondary metabolites biosynthetic gene clusters (BGCs) was  
266 made by applying antiSMASH<sup>54</sup> pipeline. The total 12399 BGCs (7804 unknown,  
267 4595 known) have been detected from 91.46% (1167) kSGBs and 66.75% (1544)  
268 uSGBs, and the BGCs coding for bacteriocin, arylpolyene, type III PKS (polyketide  
269 synthase) has appeared more than 500 times on the oral bacterial community (**Fig. 7b**,  
270 **Supplementary Table 7**). For each species' genome, the size percentage (mean:  
271 2.512%) of BGCs was calculated based on the each BGC's location on the each  
272 genome. The vast majority of the genome has a BGC range of less than 10%  
273 compared to the total genome (**Supplementary Figure 5**), included *Firmicutes*,

274 *Patescibacteria*, *Actinobacteriota*, *Proteobacteria*, etc. Notably, there represented 67%  
275 novel BGCs (2743 known, 5557 unknown) in the kSGBs and 54% novel BGCs (1852  
276 known, 2247 unknown) in the uSGBs. At the phylum level, *Elusimicrobiota*,  
277 *Actinobacteriota*, *Chloroflexota*, *Patescibacteria* contains a higher proportion of  
278 novel clusters (**Fig. 7c**). These unknown BGCSs demonstrate the enormous potential  
279 of oral microbes for the synthesis of natural metabolites for drug development and  
280 disease treatment.

## 281 **DISCUSSION**

282 In summary, we provide the largest set of oral metagenomic shotgun data,  
283 assemble tens of thousands of draft genomes for the human oral microbiome,  
284 including 2,313 new species as well as many new strains of known species. The  
285 results illustrate that culturomics have not even exhausted the microbial complexity in  
286 the more accessible body sites, and that metagenomic data for large cohorts of  
287 non-fecal samples have great potential. A number of taxa with compact genomes were  
288 identified in this study, such as CPR and Mollicutes. Mollicutes such as *Mycoplasma*  
289 and *Ureaplasma* are well known in the female reproductive tract<sup>22</sup>. Much remains to  
290 be elucidated for the metabolic requirement of small bacteria in the oral microbiome.  
291 Oral bacteria also contributed to discovery of new CRISPR-Cas systems<sup>55</sup>. Species  
292 with thousands of metagenomic and isolated genomes would be amenable to  
293 microbial GWAS<sup>56</sup> (microbial genome-wide association studies) to discover virulence  
294 factors, drug resistance and more commensal functions, which has so far only be  
295 possible for pathogens.

## 296 **Accession codes**

297 All the data are available at China National Genebank (CNGB), Shenzhen under the  
298 accession CNP0000687. <https://db.cngb.org/microbiome/>

## 299 **ACKNOWLEDGEMENTS**

300 We gratefully acknowledge colleagues at BGI-Shenzhen and China National  
301 Genebank (CNGB), Shenzhen for sample collection, DNA extraction, library  
302 construction, sequencing, and discussions.

### 303 **AUTHOR CONTRIBUTIONS**

304 J.W. initiated the overall health project, H.J. decided to include oral samples, Z.J., J.Z.,  
305 L.T. worked out the metagenomic assembly approach, with Hadoop support from X.L.  
306 M.H., Z.L., C.L. contributed Yunnan samples. P.C., K.C., X.W., Y.L. contributed  
307 4D-SZ samples, and L.S., X.T. managed the samples and data. J.Z., L.T., Z.J., H.J.  
308 interpreted the data, prepared the display items and wrote the manuscript. All authors  
309 contributed to finalizing the manuscript.

### 310 **COMPETING FINANCIAL INTERESTS**

311 The authors declare no competing financial interest.  
312

313 **ONLINE METHODS**

314 **The newly cohort and published datasets used in this study.** The 2675(2284 saliva  
315 and 391 tongue) oral metagenomics samples from Chinese 4D-shenzhen  
316 cohorts(**Supplementary Tables 1 sheet 4**) and the 671 salivary samples from six  
317 cities and villages in Yunnan province were collected in this study(**Supplementary**  
318 **Tables 1 sheet 5**), and total 706 public oral metagenomics datasets<sup>6, 23-26</sup> were  
319 downloaded from NCBI SRA databases with accession codes SRP029441,  
320 ERP006678, SRP133047, ERP110622 and SRP07256, encompassing five different  
321 studies (**Supplementary Table 1 sheet 3**) have been reported previously.

322

323 **Sample collection, DNA extraction, sequencing and quality control.** The 2955  
324 salivary samples and 391 tongue samples from Shenzhen were self-collected by  
325 volunteers, using a kit containing a room temperature stabilizing reagent to preserve  
326 the metagenome<sup>57</sup>. DNA extraction of the stored samples within the next few months  
327 was performed using the MagPure Stool DNA KF Kit B (MD5115, Magen) from  
328 1mL of each sample. Metagenomic sequencing was done on the BGISEQ-500  
329 platform<sup>58</sup> (100bp of paired-end reads for all samples and four libraries were  
330 constructed for each lane) and generated 101.4 billions pairs of raw reads. The 671  
331 salivary samples from Yunnan province were self-collected using commercial kits  
332 (Cat. 401103, Zeesan, China). Collected samples were temporarily stored in -80°C  
333 freezers and then transported to CNGB, Shenzhen with dry ice via commercial  
334 logistics (SF Express Inc.). DNA was extracted in the same way as above. Sequencing  
335 was performed on the BGISEQ-500 machines and generated 26.5 billions single-end  
336 100 bp length reads. The raw read length for each end was 100bp. After using the  
337 quality control module of metapi pipeline followed by reads filtering and trimming  
338 with strict filtration standards(not less than mean quality phred score 20 and not  
339 shorter than 51bp read length) using fastp v0.19.4<sup>59</sup>, host sequences contamination

---

340 removing using Bowtie2 v2.3.5<sup>60</sup> (hg38 index) and seqtk<sup>61</sup> v1.3, we totally got 54.9  
341 billions high-quality PE reads and 7.1 billions high-quality SE reads.

342

343 **Metagenomic De novo assembly, binning and checkm.** The high-quality PE and SE  
344 reads was individually assembled using assembly module of metapi pipeline with  
345 different max kmer cutoff by different max read length of each samples applying  
346 SPAdes v3.13.0<sup>28</sup> (PE reads with option --meta<sup>27</sup>). All configuration can see on  
347 <https://github.com/ohmeta/metapi/blob/dev/metapi/config.yaml>. After we  
348 got draft genomes on contig level of each samples, the reads was mapped back to each  
349 assemblies using BWA-MEM v0.7.17<sup>62</sup> with default parameters and calculate the  
350 contig depth by jgi\_summarize\_bam\_contig\_depths<sup>21</sup>, then using MetaBAT2  
351 v2.12.1<sup>21</sup> to do metagenomic binning individually for each samples. Finally we got  
352 totally 163,718 bins. After MAGs quality assignment by CheckM v1.0.12<sup>30</sup> lineages  
353 workflow, 15,013 high-quality (completeness > 90% and contamination < 5%, HQ)  
354 bins and 41,200 medium-quality (completeness > 50% and contamination < 10%, MQ)  
355 bins (**Supplementary Table 2**) have been generated based on MIMAG standard<sup>29</sup>.  
356 The 16S rRNA sequences in the MAGs were searched by Barrnap v0.9<sup>63</sup> with  
357 parameters "--reject 0.01 --evaluate 1e-3" and tRNA sequences in the MAGs were  
358 searched by tRNAscan-SE 2.0.3<sup>64</sup> with the default parameters.

359

360 **Public database used.** The public bacteria and archaea genomes database used in this  
361 study include (**Supplementary Table 1 sheet 6**):

362 (a) The NCBI Refseq bacteria and archaea databases

363 (<ftp://ftp.ncbi.nlm.nih.gov/genomes/refseq/>, accessed in June 2019) contain 155854

364 microbial genomes.

---

365 (b) The eHOMD<sup>31</sup> database ([http://www.homd.org/ftp/HOMD\\_prokka\\_genomes](http://www.homd.org/ftp/HOMD_prokka_genomes))  
366 contain 1526 microbial genomes come from human oral environment.

367 (c) The IGGdb<sup>15</sup> (<https://github.com/snayfach/IGGdb>) contain 23790 microbial  
368 genomes come from human gut environment.

369 (d) The hSGBRep<sup>16</sup> database contain 4930 representative microbial genomes  
370 ([http://segatalab.cibio.unitn.it/data/Pasolli\\_et\\_al.html](http://segatalab.cibio.unitn.it/data/Pasolli_et_al.html)) come from human body site  
371 include gut, oral, skin, genital tract.

372 (e) The BPUMGs<sup>14</sup> databases  
373 ([ftp://ftp.ebi.ac.uk/pub/databases/metagenomics/umgs\\_analyses/](ftp://ftp.ebi.ac.uk/pub/databases/metagenomics/umgs_analyses/)) contain 1952  
374 microbial genomes come from human gut.

375 (f) The CGR<sup>33</sup> database accession code [PRJNA482748](https://ncbi.nlm.nih.gov/submit/PRJNA482748) contain 1520 microbial  
376 genomes come from human gut bacterial culture collection.

377 (g) The HBC<sup>32</sup> database  
378 ([ftp://ftp.ebi.ac.uk/pub/databases/metagenomics/hgg\\_mags.tar.gz](ftp://ftp.ebi.ac.uk/pub/databases/metagenomics/hgg_mags.tar.gz)) contain 737  
379 microbial genomes come from human gut bacterial culture collection.

380 **Clustering metagenomic genomes into species-level genome bins.** The 56,213  
381 reconstructed genomes and 190,309 reference genomes were grouped into species  
382 -level genome bins(SGBs) by a two-step clustering strategy as reported previously<sup>16</sup>  
383 with a slight modification. In the first step, all-versus-all genetic distance matrix  
384 between the 246,522 genomes was carried out using Mash version 2.0<sup>65</sup> (“-k 21 -s 1e4”  
385 for sketching ). Then, hierarchical clustering with average linkage and 0.05 genetic  
386 distance cutoff on the distance matrix by fastcluster<sup>66</sup> was resulted to 33008 clusters.  
387 Because the Mash will underestimate the distance between the incomplete genomes<sup>67</sup>  
388 and split same-species genomes into multiple SGBs, we performed clustering base on  
389 average nucleotide identity(ANI) in the second step. First, We divide the SGB into  
390 known SGB(kSGB) and unknown SGB(uSGB) according to with or without reference

---

391 genomes. Then, a representative genome was selected for each SGBs. For the kSGB,  
392 the genome which has the largest genome size was selected. For the uSGB, all MAGs  
393 were rank by completeness(in decreasing order), contamination(increasing),  
394 coverage(decreasing), strain heterogeneity(increasing), N50(decreasing). And  
395 representative genome was selected as the one minimizing the sum of the five ranks.  
396 We recalculated the more precise genetic distance using pyani v0.2.9<sup>68</sup>(option ‘-m  
397 ANIb) for the pairs of representative genomes with mash distances less than 0.95 and  
398 only left ANI with genome coverage above 0.3. Following hierarchical clustering  
399 with complete linkage based on >95% ANI score, 12,911 representative genome  
400 which mash distances less than 0.95 were merged to 11,427 new clusters. Finally, we  
401 obtained 31,525 SGBs by two-step clustering strategy. In this dataset, only 3,589  
402 SGBs included eHMOD genomes and oral metagenomes MAGs were named Oral  
403 SGBs and can be further divided into 2,313 uSGBs and 1,276 kSGBs. The top three  
404 contributions of uSGBs are 4D\_SZ (1441 uSGBs), ZhangX\_2015 (445 uSGBs) and  
405 Yunnan (334 uSGBs).The other 27,936 SGBs are non-oral SGBs (Figure 1b).

406 **Reconstruction of the human-oral microbiome phylogenetic structure.** The  
407 phylogenetic trees of 3589 representative genomes of SGBs (Figure 3C) and 76  
408 genomes of Acholeplasmataceae Order were both built using the 400 PhyloPhlAn  
409 markers with the parameters “--diversity high --fast --min\_num\_markers 80” by the  
410 PhyloPhlAn2<sup>69</sup>. As input data for PhyloPhlAn2, proteome were predict using Prodigal  
411 v2.6.3<sup>70</sup> with default parameters. Following tools with their set of parameters were  
412 used in the configuration files:

413 Diamond v0.9.22.123<sup>71</sup> with parameters: “blastp --quiet --threads 1 --outfmt 6  
414 --more-sensitive --id 50 --max-hsps 35 -k 0”;

415 Mafft v7.407<sup>72</sup> with the “--anysymbol” option;

416 Trimal v1.4.rev15<sup>73</sup> with the “-gappyout” option;

417 Iqtree v1.6.12<sup>74</sup> with parameters: “-quiet -nt AUTO -m LG”.



418 The phylogenetic trees in figure 3c was generated using GraPhlAn v1.1.3<sup>75</sup> and the  
419 phylogenetic trees in figure 4a, figure s2 were generated using FigTree v1.4.4  
420 (<https://github.com/rambaut/figtree/releases>).

421

422 **SGBs taxonomic and function analyses.** The taxonomic classification of 3589  
423 representative genomes of SGBs was assigned using GTBD-Tk v0.3.2<sup>70, 76-79</sup>  
424 (<https://github.com/Ecogenomics/GTDBTk>) classify workflow with external GTDB  
425 database release 89.0([https://data.ace.uq.edu.au/public/gtdbtk/release\\_89/89.0/](https://data.ace.uq.edu.au/public/gtdbtk/release_89/89.0/)).  
426 Although some kSGBs already have taxonomy label, we still using GTDB-Tk to  
427 classify them because GTDB-Tk has its own taxonomy classification system that is  
428 different from the NCBI taxonomy database. Then above the genus level, we  
429 manually removed the classification tag with a single letter suffix (**Supplementary**  
430 **Table 3**). Those suffixes used to indicate that taxon needed to be subdivided based on  
431 the current GTDB reference tree. We used EggNOG mapper v1.0.3<sup>39</sup> to do  
432 genome-wide functional annotation through orthology assignment on 3589  
433 SGBs(**Supplementary table 3**) and 29 MAGs in Candidatus bgiplasma  
434 (**Supplementary Figure 2b**). The secondary metabolite biosynthesis gene  
435 clusters(BGCs) of 3587 oral bacterial genomes was identified respectively by using  
436 antiSMASH v5.0.0<sup>54</sup> with options --fullhmmer --cf-create-clusters --smcog-trees  
437 --cb-knownclusters --asf --pfam2go. Then we use the  
438 bgctk(<https://github.com/ohmeta/bgctk>) to parse and merge BGCs's results from all  
439 json file which was generated by anstiSMASH workflow.

440

441 **Mapping rate compared between different oral related genomes database.** The  
442 mapping rates of oral metagenomics reads align to three different oral related  
443 genomes databases(eHOMD, hSGB\_Rep, oralSGB\_Rep) were compared based on the  
444 statistics summary of Bowtie2's results(**Supplementary Table 4**). First we randomly

445 selected 100 oral metagenomes samples from each of 4D\_SZ and Yunnan cohorts.  
446 With all 808 public samples and 81 additional verify samples which not used to  
447 assembly (**Supplementary table 1 sheet 2**), the total 1089 oral metagenomes samples  
448 were mapped to these databases respectively using Bowtie2 v2.3.5 with default  
449 parameters. The barplot of mapping rate was generated using R package ggplot2  
450 3.1.1<sup>80</sup> faced with different databases and different country.

451

452 **Metapi for oral SGB metagenomic profiling.** The quantification of species relative  
453 abundance of oral metagenomic samples was performed with the taxonomic profiling  
454 module of metapi pipeline: i) build the oral representative SGBs' index by Bowite2; ii)  
455 align the high-quality reads of each sample to the oral genome index using Bowtie2  
456 with parameters : "--end-to-end --very-sensitive --seed 0 --time -k 2 --no-unal  
457 --no-discordant -X 1200"; iii) The normalized contigs depths were obtained by using  
458 jgi\_summarize\_bam\_contig\_depths; vi) base on the correspondence of contigs and  
459 genome, the normalized contig depth were converted to the relative abundance of  
460 each SGB for each samples. Finally we merged all representative SGBs relative  
461 abundance to generate a taxonomic profile.

462

463 **PCOA, heatmap and oral type for metapi profile.** Principal Coordinates Analysis  
464 (Pcoa) of metapi profile was done used dudi.pco function in ade4<sup>81</sup> R package based  
465 on bray distance from vegan2.5.2<sup>82</sup> R package. The mean top 10 most abundance  
466 SGBs from every study were merged (total 27 SGBs) to visual in pheatmap<sup>83</sup> R  
467 package.

468

469 **Pangenome, phylogenetic analysis of kSGB and uSGBs.** From the taxonomic  
470 profiling results of 4820 oral metagenomic samples, the most prevalent eight genus

---

471 was selected based the rank of average relative abundance(decreasing), occurrence  
472 frequency(decreasing), oral genome number / SGBs size(decreasing), include  
473 *Prevotella*, *Neisseria*, *Streptococcus*, *Veillonella*, *Porphyromonas*, *Fusobacterium*,  
474 *Pauljensenia*, *Haemophilus*. Then we choose ten most prevalent species for each  
475 genus to do pangenome analysis. First each species has a representative genome  
476 correspond to each SGBs, so we use prokka v1.13.7<sup>84</sup> to do genome annotation for all  
477 genomes of each SGBs. Then the annotated genomes were used to construct  
478 pangenome database for each SGBs via panphlan\_pangenome\_generation.py (a script  
479 come from PanPhlAn v1.2<sup>85</sup>). Finally the gene-family presence / absence profile  
480 matrix was transformed to a zero/one matrix for reference genomes and reconstructed  
481 genomes of each SGBs to do rarefaction analysis. Accumulation curves  
482 (**Supplementary Figure 3**) based on the number of core gene of each SGBs were  
483 bootstrapped ten times at each sampling interval. The observation of intra-SGB  
484 phylogenetic structure of *Neisseria* kSGB 3225, *Prevotella* kSGB 3467 and  
485 *Porphyromonas* kSGB 3273 was performed by the nonmetric multidimensional  
486 scaling analysis using the metaMDS function of R package vegan v2.5.2.

487

488 **Disease markers according to the oral genomes.** The metagenomics wise  
489 association between 3,589 metapi species profiles (SGB) and disease for previously  
490 published CRC and RA studies was done using generalized linear model (GLM) with  
491 adjust for potential confounders such as gender, age, BMI (Table S1). BMI is only  
492 available for RA. Species relative abundances was asin-sqrt transformed as described  
493 before<sup>86</sup>. Non-oral SGBs were excluded. Corrected for multiple hypothesis tests was  
494 done using FDR. We predicted disease status using gradient boosting model (GBM)  
495 in caret<sup>87</sup> R package, such that 80% of the samples were randomly sampled for each  
496 estimator. The depth of the tree at each estimator was not limited, but leaves were  
497 restricted to have at least 30 instances. We used 4000 estimators with a learning rate  
498 of 0.002. All the FDR <1% oral marker SGBs are included in the model as predictors.

499 To avoid overfitting, 5 repeat ten folds cross validation ROC was used to measure the  
500 model performance. VarImp function was used to extract the GBM importance.

501

## 502 **ACKNOWLEDGEMENTS**

503 This research was supported by the Shenzhen Municipal Government of China (),  
504 Guangdong (). We gratefully acknowledge colleagues at BGI-Shenzhen and China  
505 National Genebank (CNGB), Shenzhen for sample collection, DNA extraction, library  
506 construction, sequencing, and discussions.

507

---

508 **References**

- 509 1. Cabreiro, F. & Gems, D. Worms need microbes too: microbiota, health and  
510 aging in *Caenorhabditis elegans*. *EMBO Mol Med* **5**, 1300-1310 (2013).
- 511 2. Zhernakova, A. et al. Population-based metagenomics analysis reveals  
512 markers for gut microbiome composition and diversity. *Science* **352**, 565-569  
513 (2016).
- 514 3. Jie, Z. et al. A multi-omic cohort as a reference point for promoting a healthy  
515 gut microbiome. *To be Submitt. soon* (2019).
- 516 4. Methé, B.A. et al. A framework for human microbiome research. *Nature* **486**,  
517 215-221 (2012).
- 518 5. Lloyd-Price, J. et al. Strains, functions and dynamics in the expanded Human  
519 Microbiome Project. *Nature* **550**, 61-66 (2017).
- 520 6. Zhang, X. et al. The oral and gut microbiomes are perturbed in rheumatoid  
521 arthritis and partly normalized after treatment. *Nat Med* **21**, 895-905 (2015).
- 522 7. Qin, N. et al. Alterations of the human gut microbiome in liver cirrhosis.  
523 *Nature* **513**, 59-64 (2014).
- 524 8. Wang, J. & Jia, H. Metagenome-wide association studies: fine-mining the  
525 microbiome. *Nat Rev Microbiol* **14**, 508-522 (2016).
- 526 9. Atarashi, K. et al. Ectopic colonization of oral bacteria in the intestine drives  
527 TH1 cell induction and inflammation. *Science* **358**, 359-365 (2017).
- 528 10. Jie, Z. et al. The gut microbiome in atherosclerotic cardiovascular disease. *Nat*  
529 *Commun* **8**, 845 (2017).
- 530 11. Yu, J. et al. Metagenomic analysis of faecal microbiome as a tool towards  
531 targeted non-invasive biomarkers for colorectal cancer. *Gut* **66**, 70-78 (2017).
- 532 12. Liu, X. et al. M-GWAS for the Gut Microbiome in Chinese Adults Illuminates  
533 on Complex Diseases. *Cell* (2019).
- 534 13. Chen, T. et al. The Human Oral Microbiome Database: a web accessible  
535 resource for investigating oral microbe taxonomic and genomic information.  
536 *Database (Oxford)* **2010**, baq013 (2010).
- 537 14. Almeida, A. et al. A new genomic blueprint of the human gut microbiota.  
538 *Nature* **568**, 499-504 (2019).
- 539 15. Nayfach, S., Shi, Z.J., Seshadri, R., Pollard, K.S. & Kyrpides, N.C. New  
540 insights from uncultivated genomes of the global human gut microbiome.  
541 *Nature* **568**, 505-510 (2019).

- 
- 542 16. Pasolli, E. et al. Extensive Unexplored Human Microbiome Diversity  
543 Revealed by Over 150,000 Genomes from Metagenomes Spanning Age,  
544 Geography, and Lifestyle. *Cell* **176**, 649-662 e620 (2019).
- 545 17. Friedman, J. & Alm, E.J. Inferring correlation networks from genomic survey  
546 data. *PLoS Comput Biol* **8**, e1002687 (2012).
- 547 18. Sczyrba, A. et al. Critical Assessment of Metagenome Interpretation-a  
548 benchmark of metagenomics software. *Nat Methods* **14**, 1063-1071 (2017).
- 549 19. Alneberg, J. et al. Binning metagenomic contigs by coverage and composition.  
550 *Nat Methods* **11**, 1144-1146 (2014).
- 551 20. Backhed, F. et al. Dynamics and Stabilization of the Human Gut Microbiome  
552 during the First Year of Life. *Cell Host Microbe* **17**, 852 (2015).
- 553 21. Kang, D.D., Froula, J., Egan, R. & Wang, Z. MetaBAT, an efficient tool for  
554 accurately reconstructing single genomes from complex microbial  
555 communities. *PeerJ* **3**, e1165 (2015).
- 556 22. Jie, Z. et al. The vagino-cervical microbiome as a woman's life history. *Under*  
557 *Revis. Cell* (2019).
- 558 23. Brito, I.L. et al. Transmission of human-associated microbiota along family  
559 and social networks. *Nat Microbiol* **4**, 964-971 (2019).
- 560 24. Goltsman, D.S.A. et al. Metagenomic analysis with strain-level resolution  
561 reveals fine-scale variation in the human pregnancy microbiome. *Genome Res*  
562 **28**, 1467-1480 (2018).
- 563 25. Heintz-Buschart, A. et al. Integrated multi-omics of the human gut  
564 microbiome in a case study of familial type 1 diabetes. *Nat Microbiol* **2**, 16180  
565 (2016).
- 566 26. Zeller, G. et al. Potential of fecal microbiota for early-stage detection of  
567 colorectal cancer. *Mol Syst Biol* **10**, 766 (2014).
- 568 27. Nurk, S., Meleshko, D., Korobeynikov, A. & Pevzner, P.A. metaSPAdes: a  
569 new versatile metagenomic assembler. *Genome Res* **27**, 824-834 (2017).
- 570 28. Bankevich, A. et al. SPAdes: a new genome assembly algorithm and its  
571 applications to single-cell sequencing. *J Comput Biol* **19**, 455-477 (2012).
- 572 29. Bowers, R.M. et al. Minimum information about a single amplified genome  
573 (MISAG) and a metagenome-assembled genome (MIMAG) of bacteria and  
574 archaea. *Nat Biotechnol* **35**, 725-731 (2017).

- 
- 575 30. Parks, D.H., Imelfort, M., Skennerton, C.T., Hugenholtz, P. & Tyson, G.W.  
576 CheckM: assessing the quality of microbial genomes recovered from isolates,  
577 single cells, and metagenomes. *Genome Res* **25**, 1043-1055 (2015).
- 578 31. Escapa, I.F. et al. New Insights into Human Nostril Microbiome from the  
579 Expanded Human Oral Microbiome Database (eHOMD): a Resource for the  
580 Microbiome of the Human Aerodigestive Tract. *mSystems* **3** (2018).
- 581 32. Forster, S.C. et al. A human gut bacterial genome and culture collection for  
582 improved metagenomic analyses. *Nat Biotechnol* **37**, 186-192 (2019).
- 583 33. Zou, Y. et al. 1,520 reference genomes from cultivated human gut bacteria  
584 enable functional microbiome analyses. *Nat Biotechnol* **37**, 179-185 (2019).
- 585 34. Liu, B. et al. Deep sequencing of the oral microbiome reveals signatures of  
586 periodontal disease. *PLoS One* **7**, e37919 (2012).
- 587 35. Shi, B. et al. Dynamic changes in the subgingival microbiome and their  
588 potential for diagnosis and prognosis of periodontitis. *MBio* **6**, e01926-01914  
589 (2015).
- 590 36. Lassalle, F. et al. Oral microbiomes from hunter-gatherers and traditional  
591 farmers reveal shifts in commensal balance and pathogen load linked to diet.  
592 *Mol Ecol* **27**, 182-195 (2018).
- 593 37. Schnorr, S.L. et al. Gut microbiome of the Hadza hunter-gatherers. *Nat*  
594 *Commun* **5**, 3654 (2014).
- 595 38. Huerta-Cepas, J. et al. eggNOG 5.0: a hierarchical, functionally and  
596 phylogenetically annotated orthology resource based on 5090 organisms and  
597 2502 viruses. *Nucleic Acids Res* **47**, D309-D314 (2019).
- 598 39. Huerta-Cepas, J. et al. Fast Genome-Wide Functional Annotation through  
599 Orthology Assignment by eggNOG-Mapper. *Mol Biol Evol* **34**, 2115-2122  
600 (2017).
- 601 40. Zhang, C.C. et al. Proteomic analysis of *Deinococcus radiodurans* recovering  
602 from gamma-irradiation. *Proteomics* **5**, 138-143 (2005).
- 603 41. Fredricks, D.N., Fiedler, T.L. & Marrazzo, J.M. Molecular identification of  
604 bacteria associated with bacterial vaginosis. *N Engl J Med* **353**, 1899-1911  
605 (2005).
- 606 42. Pan, H. et al. A gene catalogue of the Sprague-Dawley rat gut metagenome.  
607 *Gigascience* **7** (2018).
- 608 43. Pan, H. et al. A single bacterium restores the microbiome dysbiosis to protect  
609 bones from destruction in a rat model of rheumatoid arthritis. *Microbiome* **7**,  
610 107 (2019).

- 
- 611 44. Nouioui, I. et al. Genome-Based Taxonomic Classification of the Phylum  
612 Actinobacteria. *Front Microbiol* **9**, 2007 (2018).
- 613 45. Mark Welch, J.L., Rossetti, B.J., Rieken, C.W., Dewhirst, F.E. & Borisy, G.G.  
614 Biogeography of a human oral microbiome at the micron scale. *Proc Natl*  
615 *Acad Sci U S A* **113**, E791-800 (2016).
- 616 46. Schmidt, T.S. et al. Extensive transmission of microbes along the  
617 gastrointestinal tract. *Elife* **8** (2019).
- 618 47. Feng, Q. et al. Gut microbiome development along the colorectal  
619 adenoma-carcinoma sequence. *Nat Commun* **6**, 6528 (2015).
- 620 48. Xu, R., Wang, Q. & Li, L. A genome-wide systems analysis reveals strong  
621 link between colorectal cancer and trimethylamine N-oxide (TMAO), a gut  
622 microbial metabolite of dietary meat and fat. *BMC Genomics* **16 Suppl 7**, S4  
623 (2015).
- 624 49. Guertin, K.A. et al. Serum Trimethylamine N-oxide, Carnitine, Choline, and  
625 Betaine in Relation to Colorectal Cancer Risk in the Alpha Tocopherol, Beta  
626 Carotene Cancer Prevention Study. *Cancer Epidemiol Biomarkers Prev* **26**,  
627 945-952 (2017).
- 628 50. Wirbel, J. et al. Meta-analysis of fecal metagenomes reveals global microbial  
629 signatures that are specific for colorectal cancer. *Nat Med* **25**, 679-689 (2019).
- 630 51. Cully, M. Microbiome therapeutics go small molecule. *Nat Rev Drug Discov*  
631 **18**, 569-572 (2019).
- 632 52. Taylor, M.R. et al. Vancomycin relieves mycophenolate mofetil-induced  
633 gastrointestinal toxicity by eliminating gut bacterial beta-glucuronidase  
634 activity. *Sci Adv* **5**, eaax2358 (2019).
- 635 53. Maier, L. et al. Extensive impact of non-antibiotic drugs on human gut  
636 bacteria. *Nature* **555**, 623-628 (2018).
- 637 54. Blin, K. et al. antiSMASH 5.0: updates to the secondary metabolite genome  
638 mining pipeline. *Nucleic Acids Research* **47**, W81-W87 (2019).
- 639 55. Shmakov, S. et al. Discovery and Functional Characterization of Diverse Class  
640 2 CRISPR-Cas Systems. *Mol Cell* **60**, 385-397 (2015).
- 641 56. Power, R.A., Parkhill, J. & de Oliveira, T. Microbial genome-wide association  
642 studies: lessons from human GWAS. *Nat Rev Genet* **18**, 41-50 (2017).
- 643 57. Han, M. et al. A novel affordable reagent for room temperature storage and  
644 transport of fecal samples for metagenomic analyses. *Microbiome* **6**, 43  
645 (2018).



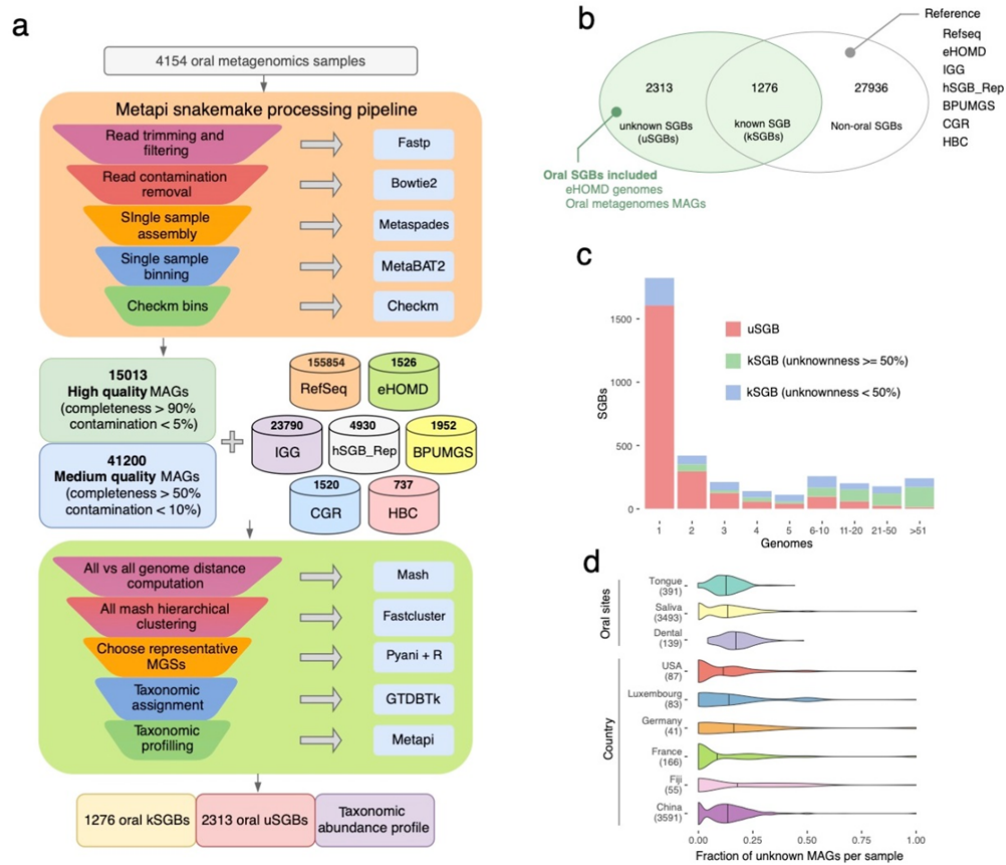
- 
- 646 58. Fang, C. et al. Assessment of the cPAS-based BGISEQ-500 platform for  
647 metagenomic sequencing. *Gigascience* **7**, 1-8 (2018).
- 648 59. Chen, S., Zhou, Y., Chen, Y. & Gu, J. fastp: an ultra-fast all-in-one FASTQ  
649 preprocessor. *Bioinformatics* **34**, i884-i890 (2018).
- 650 60. Langmead, B. & Salzberg, S.L. Fast gapped-read alignment with Bowtie 2.  
651 *Nat Methods* **9**, 357-359 (2012).
- 652 61. Shen, W., Le, S., Li, Y. & Hu, F. SeqKit: A Cross-Platform and Ultrafast  
653 Toolkit for FASTA/Q File Manipulation. *PLoS One* **11**, e0163962 (2016).
- 654 62. Li, H. & Durbin, R. Fast and accurate short read alignment with  
655 Burrows-Wheeler transform. *Bioinformatics* **25**, 1754-1760 (2009).
- 656 63. Torsten, S. barnap 0.9 : rapid ribosomal RNA prediction.  
657 <https://github.com/tseemann/barnap> (2018).
- 658 64. Chan, P.P. & Lowe, T.M. tRNAscan-SE: Searching for tRNA Genes in  
659 Genomic Sequences. *Methods Mol Biol* **1962**, 1-14 (2019).
- 660 65. Ondov, B.D. et al. Mash: fast genome and metagenome distance estimation  
661 using MinHash. *Genome Biol* **17**, 132 (2016).
- 662 66. Mullner, D. fastcluster: Fast Hierarchical, Agglomerative Clustering Routines  
663 for R and Python. *Journal of Statistical Software* **53**, 1-18 (2013).
- 664 67. Olm, M.R., Brown, C.T., Brooks, B. & Banfield, J.F. dRep: a tool for fast and  
665 accurate genomic comparisons that enables improved genome recovery from  
666 metagenomes through de-replication. *Isme Journal* **11**, 2864-2868 (2017).
- 667 68. Pritchard, L., Glover, R.H., Humphris, S., Elphinstone, J.G. & Toth, I.K.  
668 Genomics and taxonomy in diagnostics for food security: soft-rotting  
669 enterobacterial plant pathogens. *Analytical Methods* **8**, 12-24 (2016).
- 670 69. Segata, N., Bornigen, D., Morgan, X.C. & Huttenhower, C. PhyloPhlAn is a  
671 new method for improved phylogenetic and taxonomic placement of microbes.  
672 *Nat Commun* **4**, 2304 (2013).
- 673 70. Hyatt, D., LoCascio, P.F., Hauser, L.J. & Uberbacher, E.C. Gene and  
674 translation initiation site prediction in metagenomic sequences. *Bioinformatics*  
675 **28**, 2223-2230 (2012).
- 676 71. Buchfink, B., Xie, C. & Huson, D.H. Fast and sensitive protein alignment  
677 using DIAMOND. *Nat Methods* **12**, 59-60 (2015).
- 678 72. Katoh, K. & Standley, D.M. MAFFT multiple sequence alignment software  
679 version 7: improvements in performance and usability. *Mol Biol Evol* **30**,  
680 772-780 (2013).

- 
- 681 73. Capella-Gutierrez, S., Silla-Martinez, J.M. & Gabaldon, T. trimAl: a tool for  
682 automated alignment trimming in large-scale phylogenetic analyses.  
683 *Bioinformatics* **25**, 1972-1973 (2009).
- 684 74. Nguyen, L.T., Schmidt, H.A., von Haeseler, A. & Minh, B.Q. IQ-TREE: a fast  
685 and effective stochastic algorithm for estimating maximum-likelihood  
686 phylogenies. *Mol Biol Evol* **32**, 268-274 (2015).
- 687 75. Asnicar, F., Weingart, G., Tickle, T.L., Huttenhower, C. & Segata, N.  
688 Compact graphical representation of phylogenetic data and metadata with  
689 GraPhlAn. *PeerJ* **3**, e1029 (2015).
- 690 76. Matsen, F.A., Kodner, R.B. & Armbrust, E.V. pplacer: linear time  
691 maximum-likelihood and Bayesian phylogenetic placement of sequences onto  
692 a fixed reference tree. *Bmc Bioinformatics* **11** (2010).
- 693 77. Price, M.N., Dehal, P.S. & Arkin, A.P. FastTree 2-Approximately  
694 Maximum-Likelihood Trees for Large Alignments. *Plos One* **5** (2010).
- 695 78. Eddy, S.R. Accelerated Profile HMM Searches. *Plos Computational Biology* **7**  
696 (2011).
- 697 79. Jain, C., Rodriguez-R, L.M., Phillippy, A.M., Konstantinidis, K.T. & Aluru, S.  
698 High throughput ANI analysis of 90K prokaryotic genomes reveals clear  
699 species boundaries. *Nature Communications* **9** (2018).
- 700 80. Ginestet, C. ggplot2: Elegant Graphics for Data Analysis. *Journal of the Royal*  
701 *Statistical Society Series a-Statistics in Society* **174**, 245-245 (2011).
- 702 81. Bougeard, S. & Dray, S. Supervised Multiblock Analysis in R with the ade4  
703 Package. *Journal of Statistical Software* **86**, 1-17 (2018).
- 704 82. Oksanen, J. et al. vegan: Community Ecology Package. package version  
705 2.5-2. <https://CRAN.R-project.org/package=vegan> (2018).
- 706 83. Kolde, R. pheatmap: Pretty Heatmaps. R package version 1.0.12.  
707 <https://CRAN.R-project.org/package=pheatmap> (2019).
- 708 84. Seemann, T. Prokka: rapid prokaryotic genome annotation. *Bioinformatics* **30**,  
709 2068-2069 (2014).
- 710 85. Scholz, M. et al. Strain-level microbial epidemiology and population genomics  
711 from shotgun metagenomics. *Nature Methods* **13**, 435-+ (2016).
- 712 86. Morgan, X.C. et al. Dysfunction of the intestinal microbiome in inflammatory  
713 bowel disease and treatment. *Genome Biology* **13** (2012).
- 714 87. Kuhn., M. et al. caret: Classification and Regression Training. R package  
715 version 6.0-84. <https://CRAN.R-project.org/package=caret> (2019).

716

717

718 **Figures**



719

720 **Figure 1. 3,589 oral SGBs assembled from 4154 (3346 new sequence)**

721 **meta-analyzed oral-wide metagenomes.**

722 **a**, Species genome bins construction workflow. **b**, Overlap of oral assembled genomes

723 and reference genomes. kSGBs contains both existing microbial genomes (including

724 other metagenomic assemblies) and genomes reconstructed here. uSGBs are only

725 genomes reconstructed here and without existing isolate or metagenomically

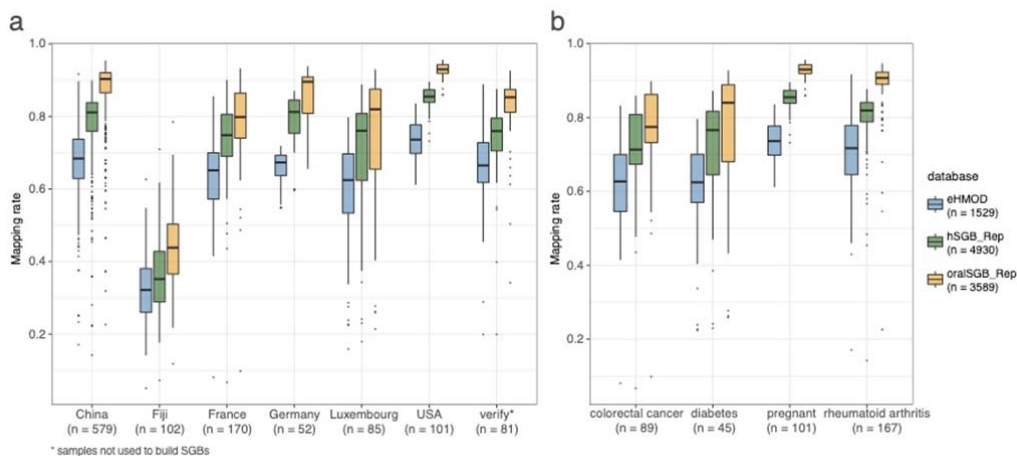
726 assembled genomes. Non-oral SGBs contains kSGBs that are not sourced from human

727 oral samples. **c**, Genome numbers distribution of uSGBs and kSGBs. **d**, Distribution

728 of the fraction of uMAGs in each sample by oral sites and country.

729

730



731

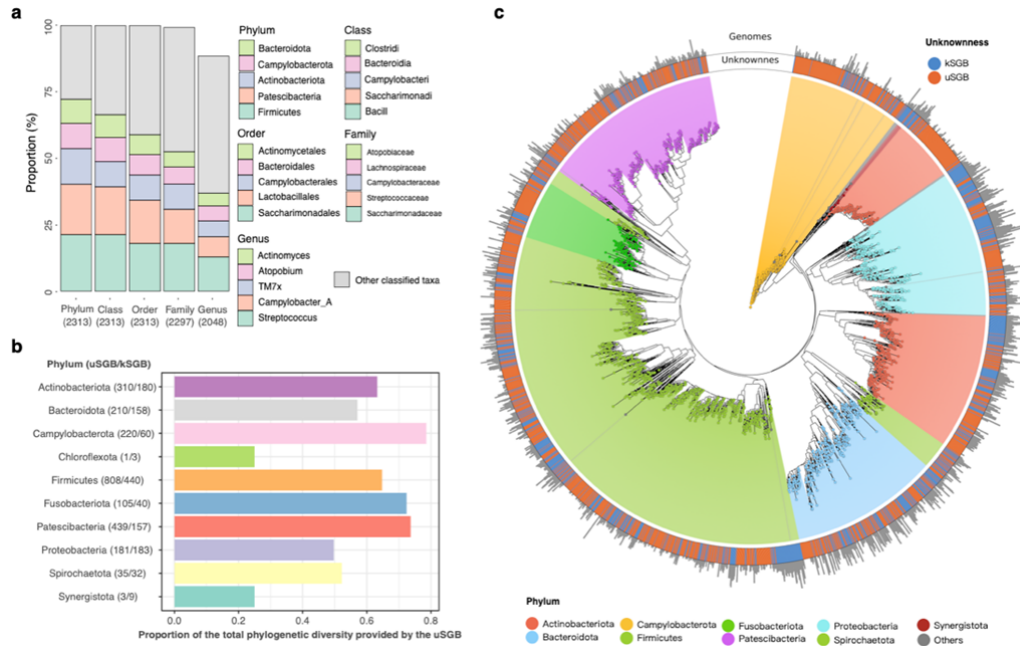
732 **Figure 2. The expanded genome set substantially increases the mappability of**  
733 **oral metagenomes.**

734 The raw reads from all the 808 public samples, 100 subsampled of 2674 China  
735 Shenzhen and 671 China Yunnan, and 81 additional verify samples which not used to  
736 build SGBs were mapped against eHMOD, representative human SGBs (hSGB\_Rep)  
737 and representative oral SGBs (oralSGB\_Rep). Among three databases, our  
738 representative oral SGBs have the highest raw-read mappability in all country and  
739 verify datasets.

740

741

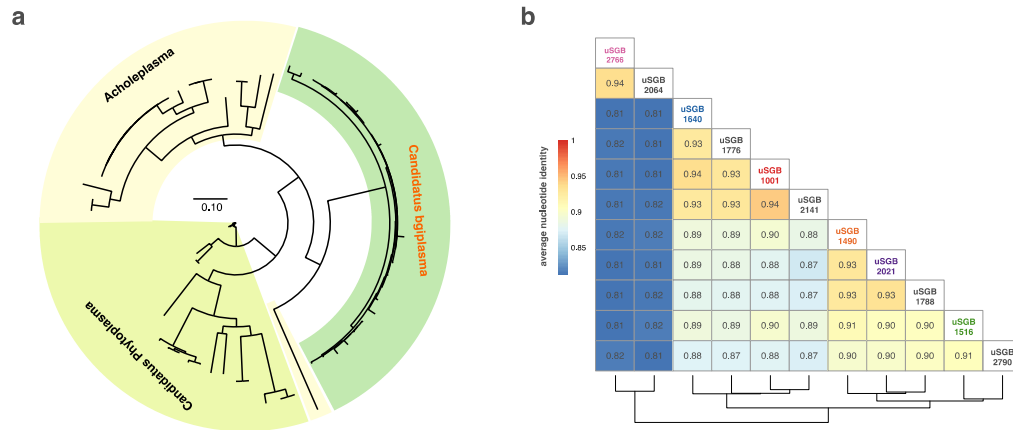
742 **Figure 3. Phylogeny of representative oral SGBs**



743

744 **a**, Taxonomic composition of the 2,313 uSGB, Only the five most frequently  
 745 observed taxa are shown in the legend, with the remaining lineages grouped as “other  
 746 classified taxa”. **b**, Proportion of the total phylogenetic diversity provided by the  
 747 uSGB. **c**, oral-associated microbial phylogenetic tree of representative genomes from  
 748 3589 species-level genome bin (SGB).

749

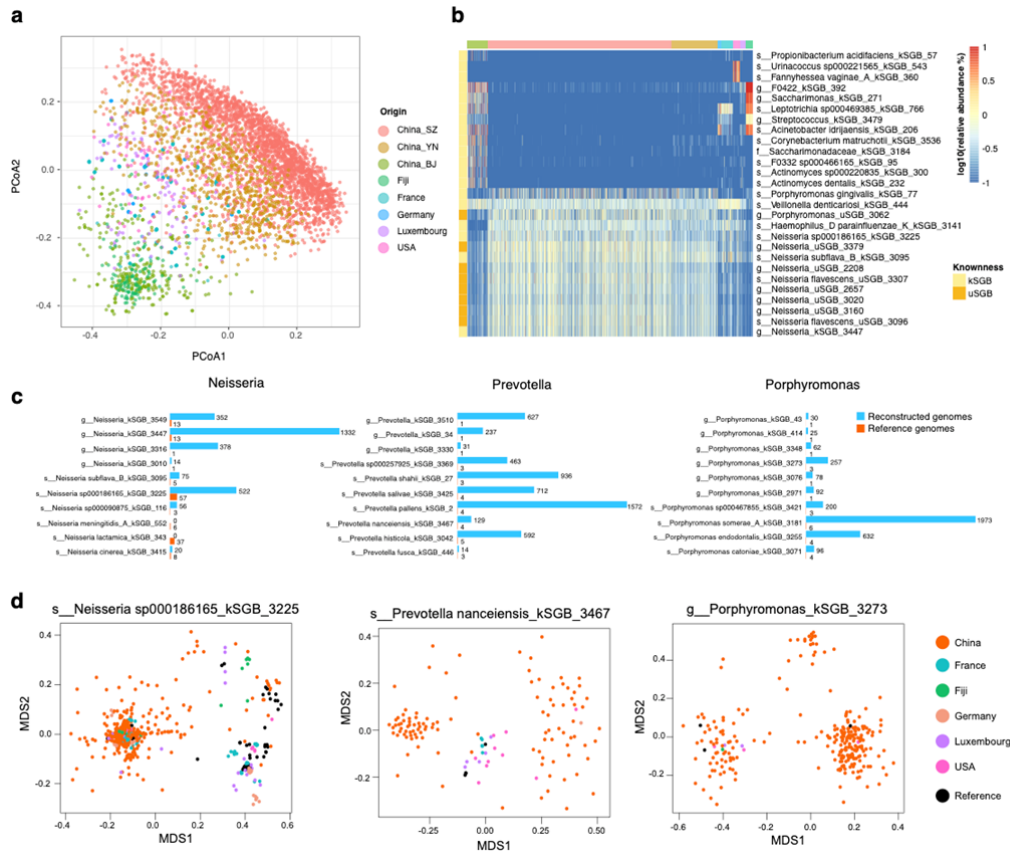


750

751 **Figure 4. A new candidatus family is found within the Acholeplasmataceae**  
 752 **Order.**

753 **a**, phylogenetic tree from all MAGs in the new candidatus family(Candidatus  
 754 bgiplasma) and known genomes in Acholeplasmataceae Order. Supplementary Figure  
 755 2a reports the detail of phylogenetic tree in Candidatus bgiplasma. **b**, Average  
 756 nucleotide identity(ANI) between all uSGB in the *Ca.* bgiplasma represent clearly two  
 757 genus clades which ANI less than 0.85. Unknown SGBs without HQ MAGs are left  
 758 black.

759



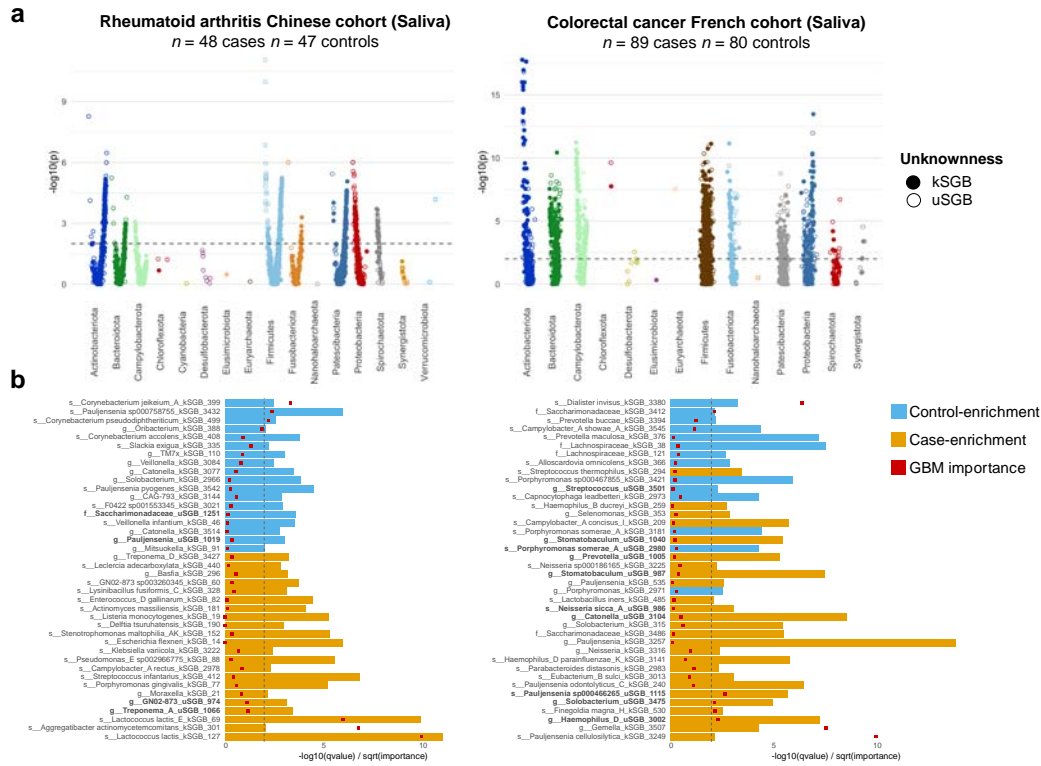
760

761 **Figure 5. Geographical distribution of oral SGBs and strains.**

762 **a**, Principal coordinate analysis plot based on Bray-Curtis distances of oral SGB  
 763 relative abundance profile highlights distinct microbial communities among different  
 764 origin populations. **b**, The relative abundance of top 10 most abundance SGBs from  
 765 each origin populations. A large set of reconstructed uSGBs are widely high  
 766 abundance distribution in our cohort (Shenzhen and Yunnan) and lack of several  
 767 highly abundant kSGBs in other population. Species are order by hclust with  
 768 complete linkage and euclidean distance. **c**, Our reconstructed MAGs largely extend  
 769 the size (genome numbers) of the top 10 most abundance species from common oral  
 770 genus with few reference genomes. **d**, Multidimensional scaling on average  
 771 nucleotide identity between MAG and reference genomes in species showed strain  
 772 variety and that constructed MAGs dominated the sub species. Only HQ MAGs and  
 773 reference genomes are showed.





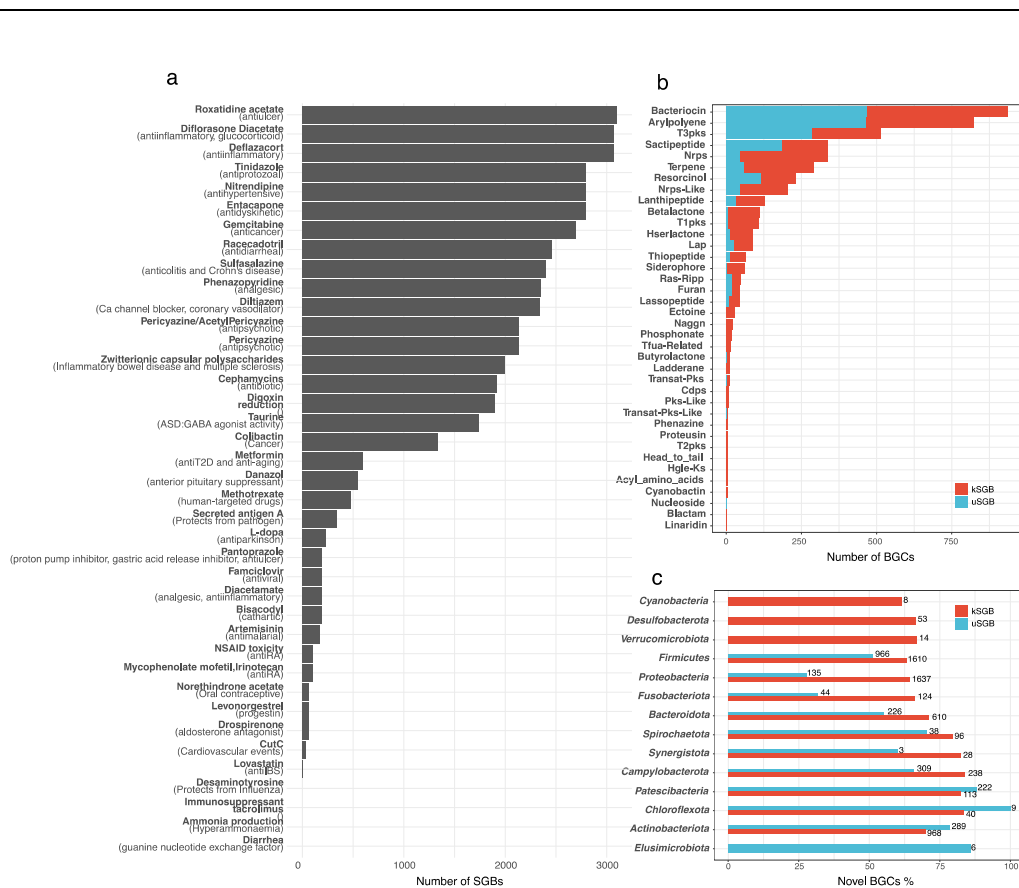


775

776 **Figure 6. Disease markers according to the oral genomes.**

777 **a**, The Manhattan plot shows metagenomic wise association of oral SGBs for RA and  
 778 CRC studies. The species are ordered according to their phylogeny (bottom) and the  
 779 association direction (positive or negative). Each point is one SGB and point height  
 780 indicates the FDR value correction for multiple hypothesis tests from a generalized  
 781 linear model (GLM) test between diseased and healthy species abundance after  
 782 adjusting Age, Gender, BMI. The dotted line indicates a false discovery rate (FDR) of  
 783 1%. **b**, SGBs association with RA and CRC. We select 40 large and most importance  
 784 oral SGBs (>10 genomes) for disease prediction using Gradient Boosting Machine  
 785 (GBM). The species are order according to their partial spearman correlation adjusted  
 786 age, gender, BMI and GBM importance. The bar length indicated the FDR value  
 787 between groups as described above. The dotted line indicates a false discovery rate  
 788 (FDR) of 1%. The red square in bar is the sqrt GBM importance. uSGBs are highlight  
 789 in bold label text.

790



791

792 **Figure 7. A comprehensive mapping of the function repertoire of the human oral**  
 793 **microbiome.**

794 **a**, Number of oral SGBs who share homologous to gut microbiome enzyme coding

795 drug metabolite or healthy related function. Details see Supplementary Table 6. **b**,

796 Summary of predicted BGCs in oral microbiome. Numbers of BGC of 38 different

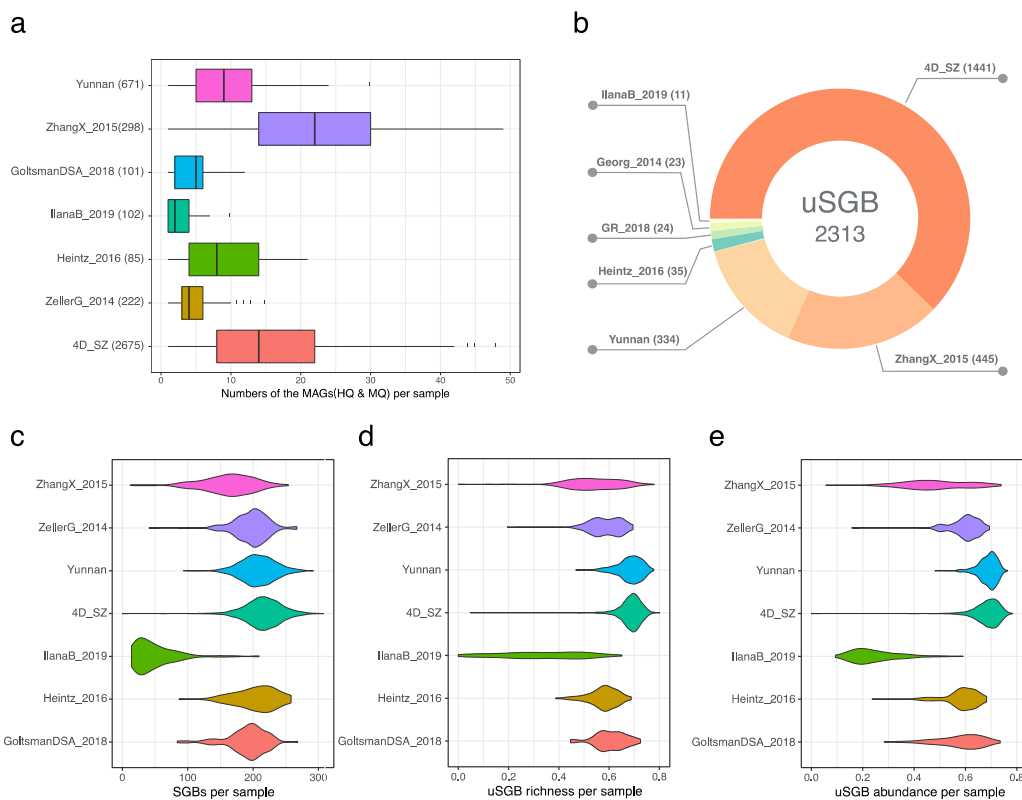
797 types detected in the 2711 oral bacterial genomes were grouped by kSGB and uSGB.

798 **c**, Fraction of novel BGCs across phylum levels. The numbers of bar show the novel

799 BGC count while bar length represent kSGBs/uSGBs ratio on the phylum levels.

800

801 **Supplementary Figures**

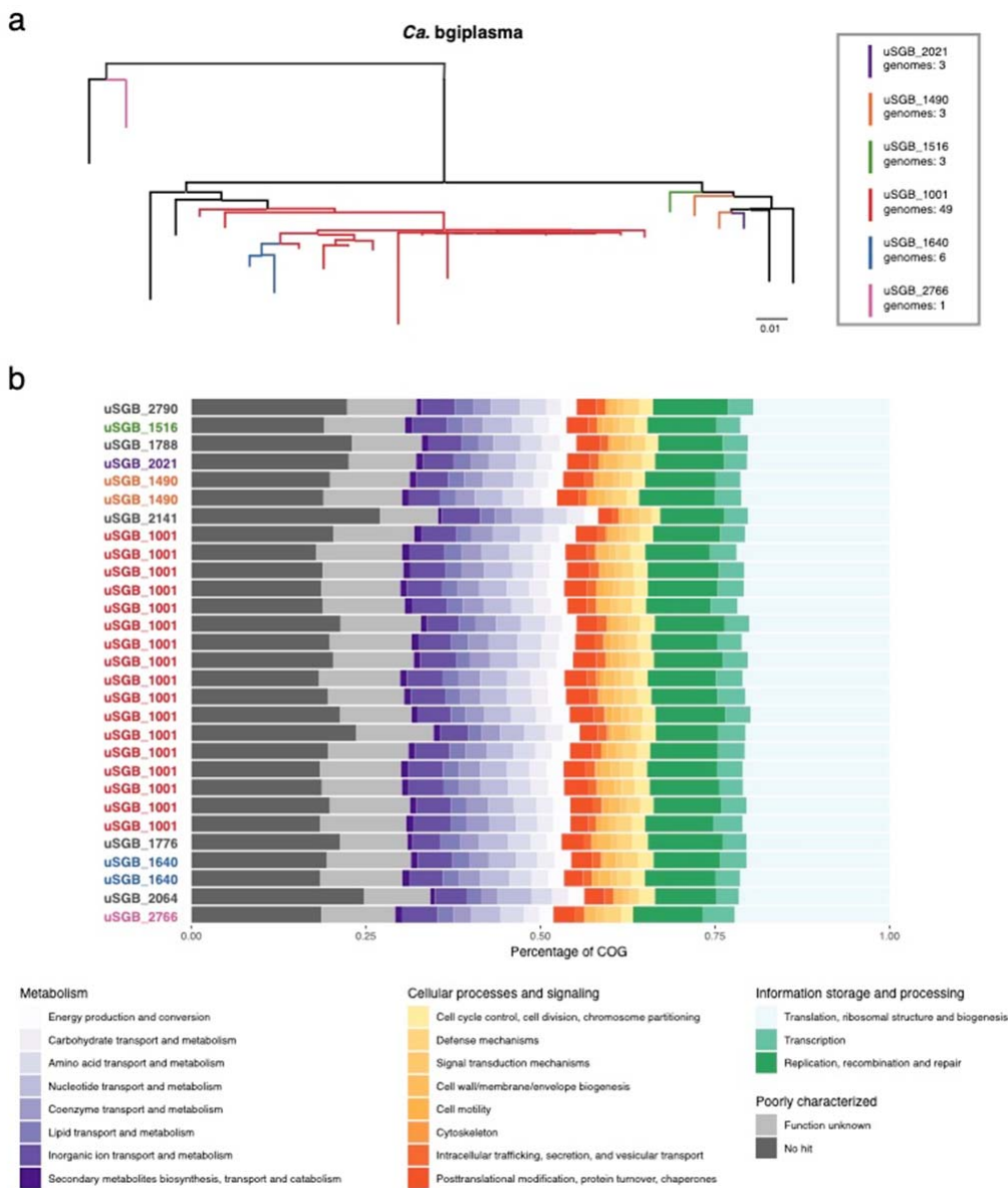


802

803 **Supplementary Figure 1. Summary of assembly quality, SGBs distribution**  
804 **across 7 studies.**

805 **a**, Numbers of medium quality and high quality MAGs in samples from 7 studies. **b**,  
806 3,589 uSGBs origin distribution across studies. **c**, The number of all SGBs (>0.001  
807 abundance) for each samples. **d**. uSGB richness (number of uSGB/number of all SGB)  
808 for each sample. **e**. Sum of all uSGB abundance for each samples.

809



810

811 **Supplementary Figure 2. Phylogenetic tree and COG functional annotation from**  
812 **all MAGs in the new candidatus family.**

813 **a**, A phylogenetic tree from *Ca. bgiplasma* (**Fig. 4a**) are displayed detailed here. The

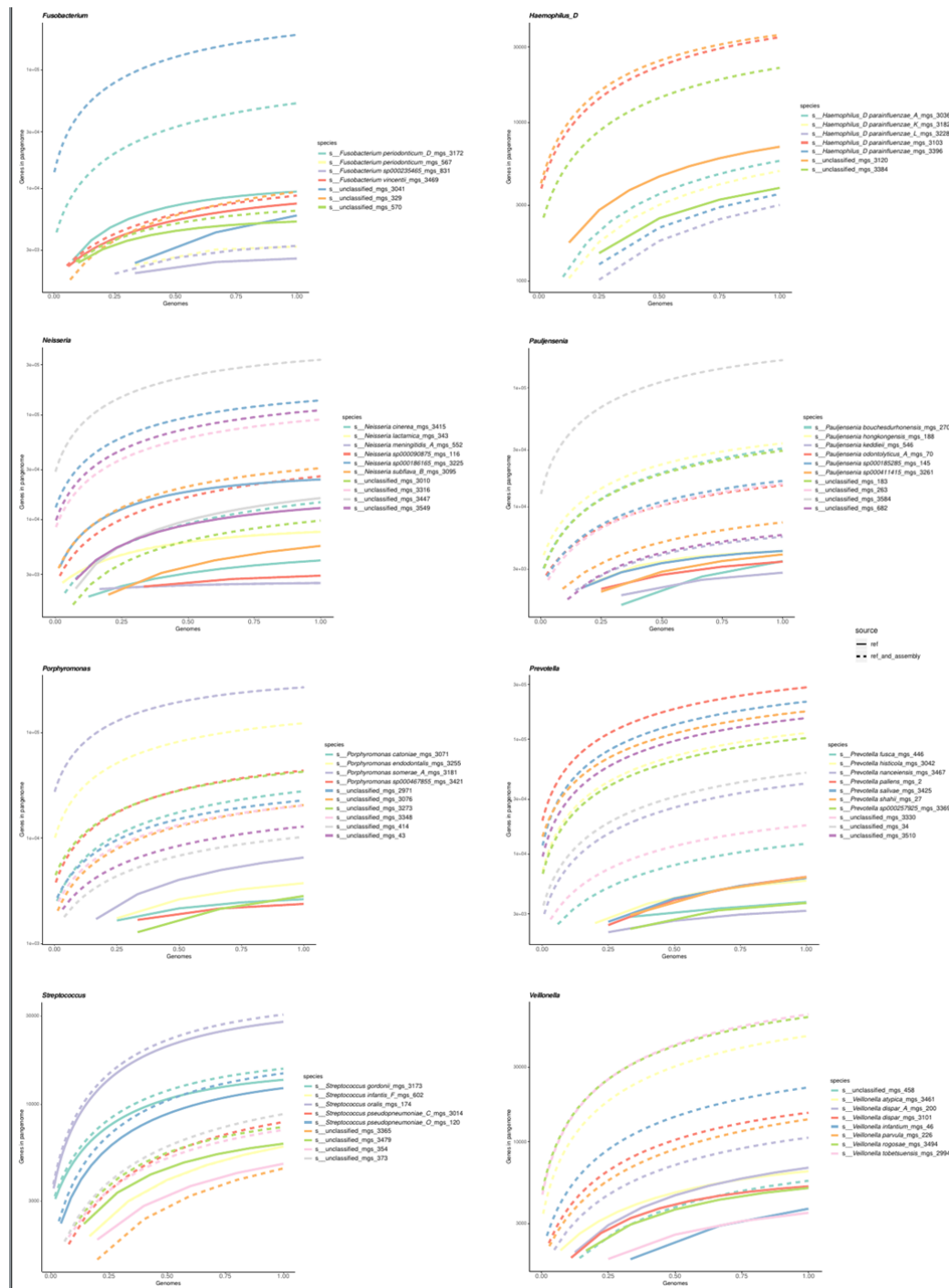
814 high quality MAGs belong the same species are colored the same color and medium

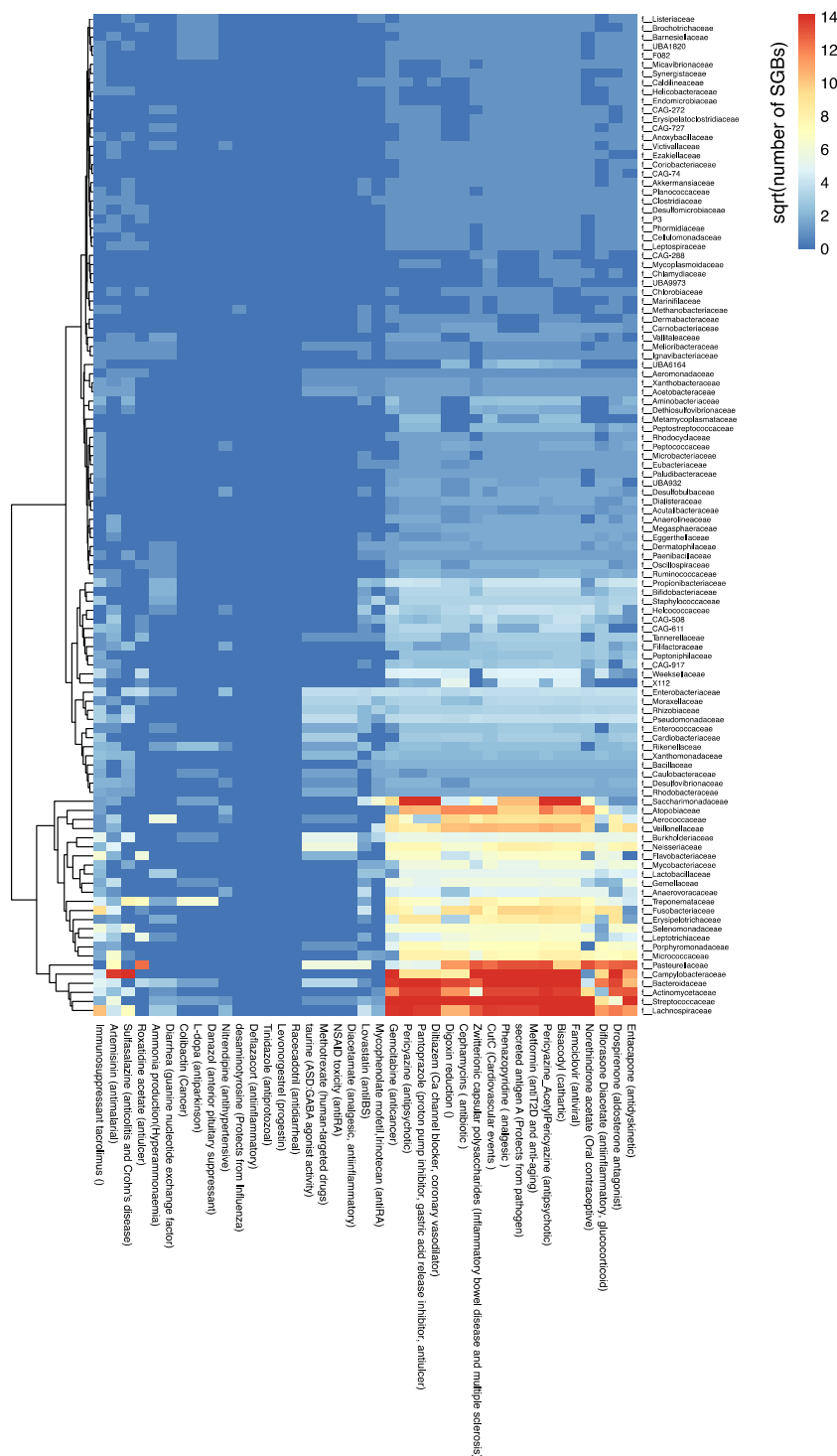
815 quality MAGs are left black. **b**, *Ca. bgiplasma* function genome annotated by

816 EggNOG mapper. The main function category of COG are displayed as the

817 percentage of genes annotated to that category.

818





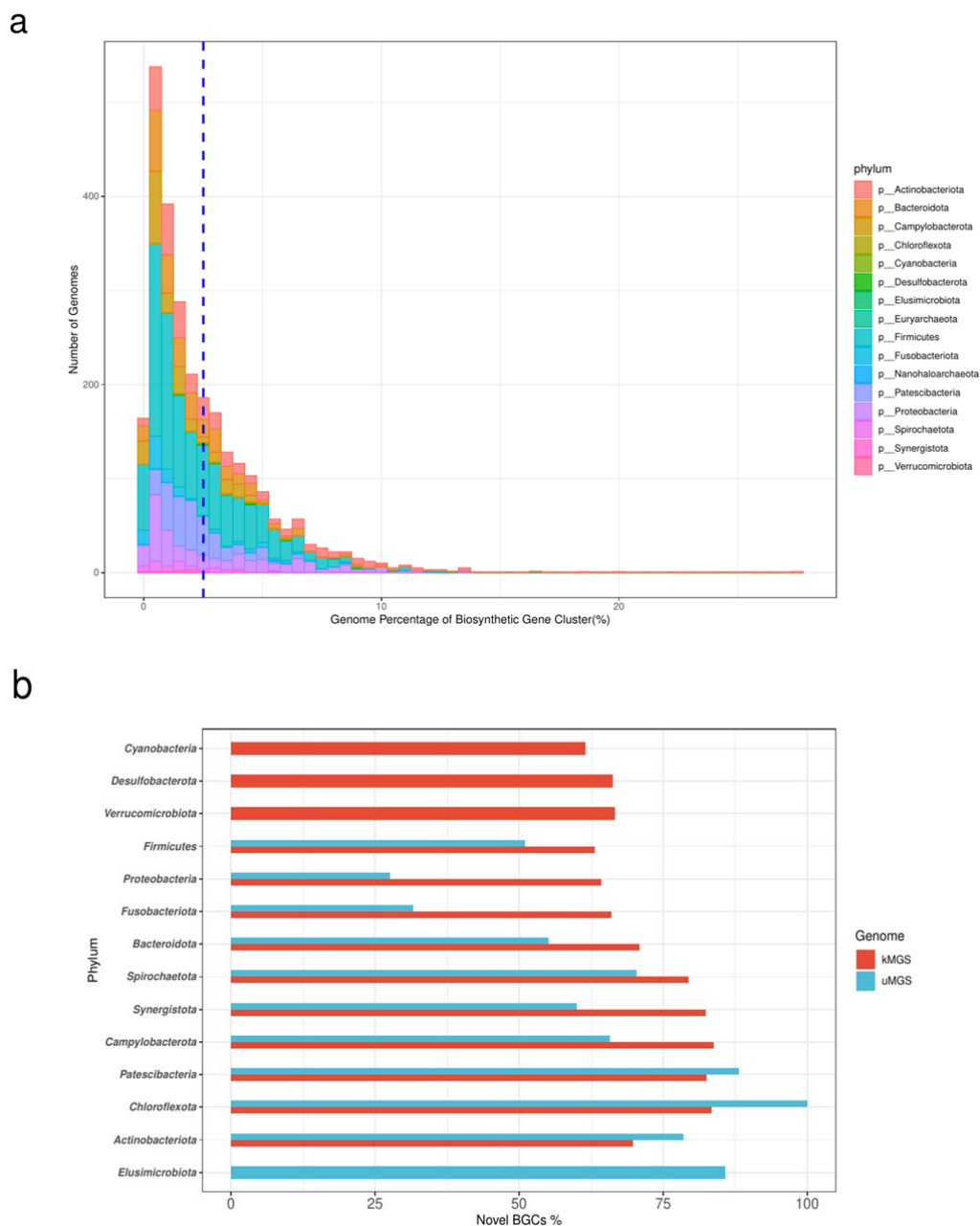
825

826 **Supplementary Figure 4. Heatmap of number of SGBs at family level who share**

827 **homologous to gut microbiome enzyme coding drug metabolite or healthy**

828 **related function.**

829 Cell is sqrt number of SGBs. Hclust with canberra distance.



830

831 **Supplementary Figure 5. The detection of BGCs on the human oral microbiome**

832 **a**, The distribution of genome percentage of biosynthetic gene cluster. From oral  
833 microbiome included 2713 genomes form 16 different phylum. The x coordinate  
834 corresponds to the proportion of BGC size, and the y coordinate corresponds to the  
835 number of genomes. The blue vertical line indicates the average proportion of BGC  
836 size: 2.512%. **b**, Novel BGCs proportion on phylum level of oral microbiome. The x



837 coordinate corresponds to the proportion of the number of the novel BGCs, the y

838 coordinate corresponds to the 14 different phylum grouped by uSGB and kSGB.

839